Characterization and activity of copper-on-carbon catalysts for low-temperature selective reduction of nitric oxide with ammonia

Naoya Shigemoto * and John B. Moffat **

Department of Chemistry and the Guelph-Waterloo Centre for Graduate Work in Chemistry and Biochemistry, University of Waterloo, Waterloo, Ontario, Canada N2L 3G1

Received 11 May 1999; accepted 6 July 2000

The activities for NO reduction with ammonia in the presence and absence of O_2 have been examined over copper salts supported on activated carbon (AC) and carbon black (CB) which have been characterized by application of X-ray diffraction and scanning electron microscopy before and after use in the reduction process. The beneficial effects of increases in loading and the introduction of oxygen are demonstrated. On the most active catalyst and under optimum conditions 100% reduction of the NO to N_2 occurs at 180 °C and Cu, Cu_2O and CuO on the catalyst are shown to be present at various stages of the preparation and reduction process with large crystallites of metallic copper detected on the AC catalyst of optimum loading. Deactivation and regeneration of the catalysts is also examined. A mechanism for the redox process is proposed.

Keywords: copper/carbon, reduction, nitric oxide

1. Introduction

Nitrogen oxides (NO_x), well known environmentally disadvantageous noxious vapours, are found in the effluent from both stationary and mobile sources [1–3]. Although a variety of processes has been proposed for the removal of these noxious vapours from atmospheric emissions [1] and a number of these has been commercialized there is evidence that the production of NO_x is increasing [1,4]. Both selective catalytic reduction (SCR) and selective non-catalytic reduction (SNR) processes have been proposed, but that employing vanadia/titania catalysts has received the widest application to stationary sources at least at temperatures between 300 and 600 °C [1–4,6–12], while noble metals with added ceria are employed in automobile exhaust systems [13–15].

Noble metals (Pt, Pd, Rh) or metal oxides (for example, CuO, Fe_2O_3, MnO_2, NiO, MoO_3, V_2O_5) supported on suitable porous solids (for example, TiO_2, Al_2O_3, SiO_2, zeolites) have high catalytic activity for the selective reduction of NO to N_2 with NH_3 at relatively high reaction temperatures (greater than 573 K) [1–3,16–21]. In contrast, activated carbon (AC) [22,23] and AC-based catalysts supporting copper salts [16,24,25], iron oxide [26–28] or vanadium oxides [29,30] are effective for the reduction process at lower temperatures. Although the results of numerous studies of the reduction of NO on various carbon-based catalysts have been reported, relatively few papers have been concerned with the morphological and crystallographic state of metal salts dispersed on carbon [31–34].

In the impregnation process, particularly in the drying stage, in which an aqueous solution of a metal salt is contacted with a carbonaceous material, it is anticipated, due to the hydrophobic nature of the surface of carbon, that aqueous drops of the solution move toward relatively wide pores [35] and the metal salts become packed in such pores. Consequently, the carbon supports may provide advantageous dispersions of metal salts on the carbon surface.

The oxidation/reduction cycle of catalytic metal species is important in maintaining the steady activity for NO reduction with ammonia. Metal halides have been noted as active metal species for NO reduction, although the role of the halide in the oxidation/reduction cycle is not yet understood [20]. In the present work activities for NO reduction with ammonia have been examined for catalysts with various loadings of copper salts on a number of carbon supports such as AC or carbon black (CB) to elucidate the supporting effect of active metal compounds on carbons. The carbon catalysts before and after use for NO reduction have been characterized by X-ray diffraction (XRD) and scanning electron microscopy (SEM), particularly focusing on the supported state of the catalytic metals on carbon materials. The active copper species for NO reduction with ammonia are also proposed.

2. Experimental

2.1. Preparation of catalysts

Three carbon materials were employed as supports. Activated carbon prepared from coals (AC, KINTALR GA-2, Cataler Industry Inc., Japan; surface area = 1576 m^2/g, 10–20 mesh), carbon black (CB, BLACK PEARLSR 20004R,

* On leave from Shikoku Research Institute Inc., 2109 Yashima-nishimaci, Takamatsu 761-01, Japan.
** To whom correspondence should be addressed.

Cabot Corp., Canada; surface area = 1270 m^2/g) and unburned carbon ash (UC; surface area = 20.9 m^2/g) collected from a hopper of an electric precipitator at an oil-fired power plant.

The catalysts were prepared by pore volume impregnation with aqueous solutions of the metal salts, and dried at 373 K over a boiling-water bath. For the formation of tetraaminecopper(II) nitrate ($[Cu(NH_3)_4](NO_3)_2$), an excess of aqueous ammonia was added to $Cu(NO_3)_2{\cdot}3H_2O$. For the preparation of copper hydroxide/AC catalysts, an aqueous solution of copper nitrate was added to AC, dried at 373 K followed by addition of aqueous ammonia. After washing with water the impregnated AC particles were filtered and dried as noted above. The catalysts thus prepared are labelled by the preparative materials, for example, 10% $Cu(NO_3)_2$/AC, in which the weight ratio of salt as metal to AC is indicated. All reagents of analytical grade were used as received.

2.2. Measurement of NO reduction activity

The activities of the carbon catalysts were examined using a fixed-bed reactor (glass tube, 4 mm inside diameter) at 393, 423 and 453 K. A reactant gas mixture of ca. 3.0% NO and 3.6% NH_3 (occasionally 6.0% O_2 was added) in a 100 ml/min flow of helium was passed through 0.25 g of catalyst which had been previously dried and heated at 523 K in a helium stream (50 ml/min) for 1 h. A small volume of the effluent from the reactor was periodically introduced into a gas chromatograph (Hewlett Packard 5890) fitted with a TCD and a column packed with molecular sieve 5A (Chromatographic Specialties Inc., 60/80 mesh, 1 mm $\times$ 1.0 m, 313 K) to determine the quantities of N_2 produced. Since the quantities of nitrogen oxides such as N_2O and NO_2 found in the reactor effluent were generally very small under the conditions employed and with 10% $Cu(NO_3)_2$/AC, analyses for these gases were carried out only when deemed necessary. Measurements were carried out after steady state had been reached, usually within one hour. NO, NH_3, O_2 and He were obtained from Linde and were used as received.

The conversion of NO into N_2 is defined as effluent N_2/feedstream NO and is taken as the activity for the reduction of NO. The activity at 1 h time-on-stream is employed to compare the efficiency of the catalysts, unless otherwise stated.

2.3. Characterization of the catalysts

Powder X-ray diffraction measurements employed an MXP system (MAC Science Co., Tokyo) with Cu Kα radiation. Crystallite size for a given diffraction face of copper salts on AC was calculated by application of Sherrer's equation [36].

Scanning electron microscopy employed a JXA 840A electron probe microanalyzer (JEOL, Tokyo) with samples gold coated in vacuum.

BET surface areas and pore size distributions were calculated by application of the Cranston–Inkley method [37] to N_2 adsorption/desorption isotherms obtained at 77 K using a BELSORP 28SA (BEL Japan Inc., Osaka).

3. Results

3.1. Pore size distributions

Pore size distributions show substantial differences among the three carbons (figure 1). AC and CB contain small mesopores of radii less than approximately 2.5 nm, consistent with their high surface areas, while UC appears to be essentially devoid of a porous structure.

3.2. Temperature dependence of NO reduction activity

Figure 2 shows the temperature dependence of NO reduction activity for Cu, Fe, Co and Ni nitrate impregnated on AC as well as the support itself as a reference. For all catalysts shown in this figure the activity for NO reduction with NH_3 increased with increasing reaction temperature, whereas AC showed a low activity in the range of reaction temperature employed. In particular, Cu/AC and Fe/AC catalysts exhibited significantly higher conversions of NO to N_2 (24 and 18% at 453 K, respectively) than those found for Co/AC and Ni/AC.

3.3. The activity of various copper and iron salts on AC

Table 1 shows the NO reduction activity over copper and iron salts impregnated on AC, at a reaction temperature of 453 K and metal loadings of 10 wt%. $Cu(NO_3)_2$/AC and $Cu(OH)_2$/AC produced 24% conversion of NO to N_2 and the copper amine complex, $[Cu(NH_3)_4](NO_3)_2$/AC showed

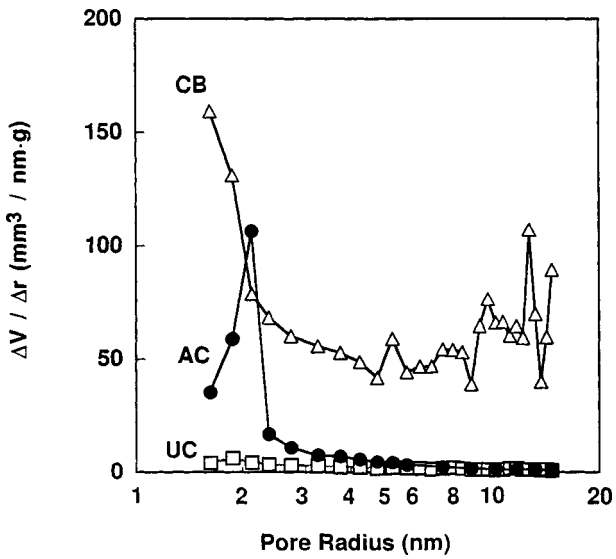

Figure 1. Pore size distribution curves; (●) activated carbon (AC); (△) carbon black (CB); (□) unburned carbon ash (UC).

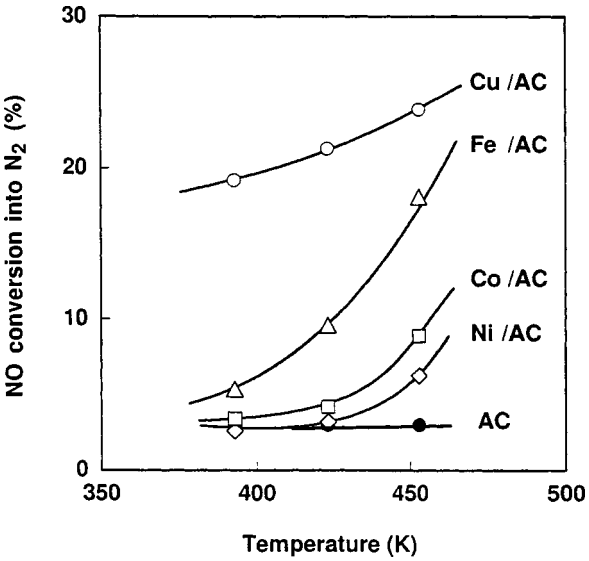

Figure 2. Temperature dependence of activity for NO reduction with NH_3 over AC (●) and metal nitrate supported on AC; (○) Cu; (△) Fe; (□) Co; (◇) Ni; reactant gas, NO (3.0%) + NH_3 (3.6%) in He; metal loading amount, 10 wt% as metal; reaction time 1 h.

Table 1
The activities for NO reduction with NH_3 for metal salts supported on activated carbon. [a]

Metal salt	Conversion into N_2 (%)
$Cu(NO_3)_2$	23.9
$Cu(OH)_2$	23.4
$[Cu(NH_3)_4](NO_3)_2$	35.0
$CuCl_2$	8.5
$CuSO_4$	8.4
$Cu(CH_3COO)_2$	4.3
$Fe(NO_3)_3$	18.1
$FeCl_3$	8.4
$FeSO_4$	4.7
Activated carbon	3.1

[a] Reaction conditions: temperature 453 K, NO 3.0%, NH_3 3.6%, reaction time 60 min, metal/C 0.10 (w/w).

the highest activity (35% conversion) of those catalysts employed, where these copper salts or complex may be transformed into CuO by the pretreatment at 523 K in helium. The activities of $CuCl_2$/AC and $CuSO_4$/AC were substantially lower than those observed with $Cu(NO_3)_2$/AC, while copper acetate/AC has an activity similar to that for AC itself.

With the iron salts on AC only $Fe(NO_3)_3$ showed relatively high activity for NO reduction, with considerably smaller activities found with $FeCl_3$/AC and $FeSO_4$/AC.

3.4. Effect of copper loading amount

Figure 3 compares the effect of copper loading on various carbon supports with the activity for NO reduction. The activity for $Cu(NO_3)_2$/AC increased linearly with increasing weight per cent of Cu in the catalyst, reached a maximum conversion to N_2 of 81% at approximately 40% of Cu loading, and then decreased slightly at a higher loading of 60%. In contrast, with copper supported on CB the activity increased with Cu loading at low Cu loadings (<10 wt%), and reached a plateau of approximately 20% conversion at higher Cu loadings (>10 wt%). No activity for NO reduction was observed for copper supported on UC regardless of the Cu loading.

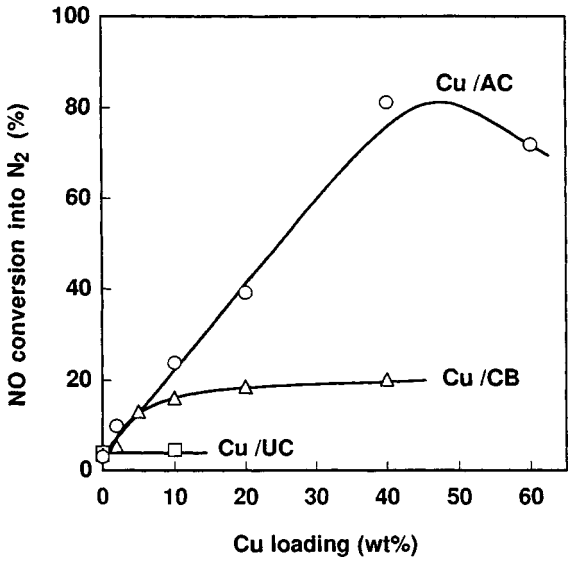

Figure 3. Effect of Cu loading amount on activity for NO reduction with NH_3 over AC (○), CB (△) and UC (□) supports; reaction temperature, 453 K; other conditions as in figure 2.

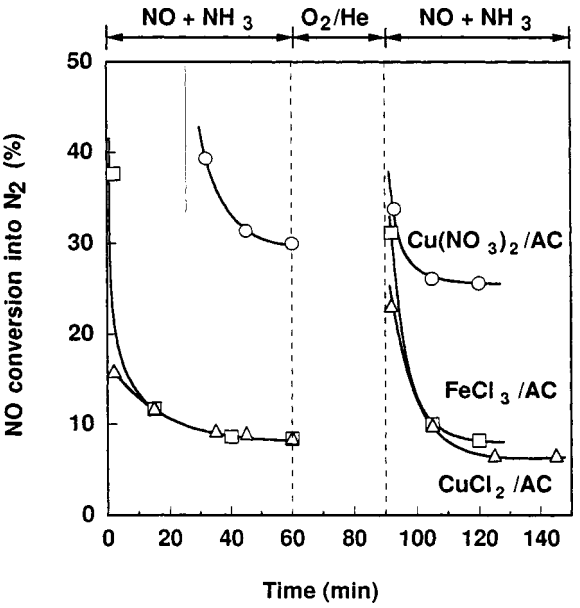

Figure 4. Transition behaviour of activity for NO reduction before and after O_2 treatment over $Cu(NO_3)_2$ (○), $CuCl_2$ (△) and $FeCl_3$ (□) on AC; O_2 treatment, 6.0% O_2/He at 453 K; other reaction conditions as in figure 3.

3.5. Catalyst deactivation and regeneration by O_2 treatment

With $Cu(NO_3)_2$/AC catalysts the NO reduction activity decreased with reaction time and approached a relatively

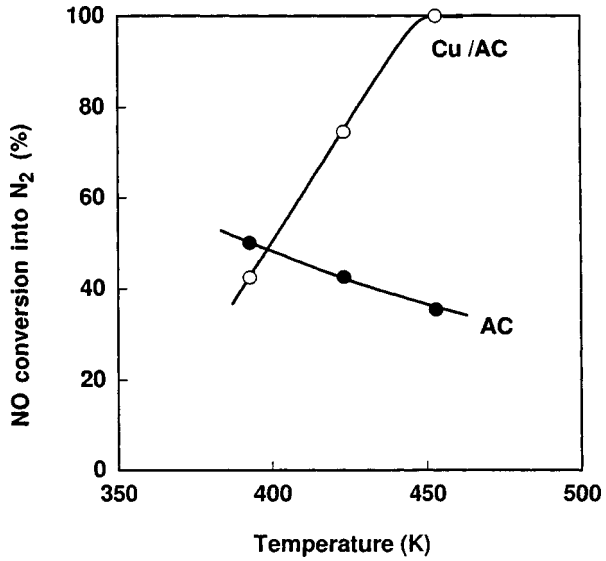

Figure 5. Temperature dependence of activity for NO reduction with NH_3 in presence of O_2 over AC (•) and $Cu(NO_3)_2$-on-AC (○); reactant gas, NO (3.0%) + NH_3 (3.6%) + O_2 (6.0%) in He; other reaction conditions as in figure 2.

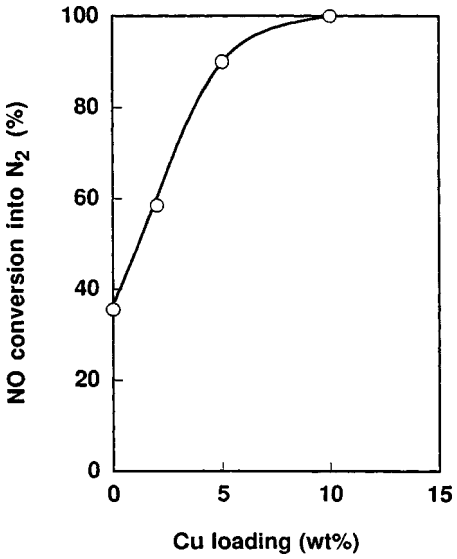

Figure 6. Effect of Cu loading amount on activity for NO reduction with NH_3 in presence of O_2 over $Cu(NO_3)_2$-on-AC (○); reaction conditions as in figure 5.

high, steady value after ca. 1 h. Similar but more precipitous deactivation of the AC catalysts prepared from copper chloride and iron chloride was observed with plateaus reached at considerably lower values of the conversion than found with $Cu(NO_3)_2$/AC.

After exposing the deactivated catalysts to an O_2/He flow at 453 K for 0.5 h the activities improved but again suffered deactivation on further exposure to NO and NH_3. It is of interest to note that the deactivation behaviour of the copper-based catalysts either before or after O_2 regeneration is strongly dependent on the preparative reagents.

3.6. NO reduction with NH_3 in presence of O_2

As has been noted [18] by others the conversion of NO with NH_3 on supported copper catalysts is markedly altered on introduction of oxygen. The activity of AC itself is relatively high at low temperatures but decreased with increasing reaction temperature (figure 5). In contrast, the activity of $Cu(NO_3)_2$/AC increased monotonously with increasing reaction temperature in agreement with the results in the literature [16], reaching a conversion of 100% at 453 K. These results may be compared with those from a recent study of the reduction of NO with NH_3 over V_2O_5–MoO_3/TiO_2 catalysts in which the conversion of NO to N_2 was approximately 35% at 475 K, increasing to nearly 100% at 550 K [38]. A comparison with the results in figure 2, where O_2 was absent, shows that the presence of O_2 in the reactant gas promotes the activity for NO reduction with NH_3. Such enhancement of NO reduction with NH_3 by O_2 has been observed with many catalysts [1,3].

A comparison of the effect of the loading of Cu on AC with and without O_2 is of interest (figure 6 and compare figure 3). It is clear that the introduction of O_2 provides a substantial enhancement such that, in its presence, a complete conversion of NO is achieved at a loading of 10%, while in its absence the conversion at the same loading is only 25%.

3.7. XRD analysis of the carbon catalysts

Powder XRD patterns obtained for activated carbon and carbon black show that both supports are amorphous (figures 7(a) and 8(a). Sharp peaks, assignable to $Cu_2(OH)_3NO_3$, are clearly evident in the patterns for $Cu(NO_3)_2$/AC and $Cu(NO_3)_2$/CB after the impregnation (figures 7 (b), (d) and 8 (b), (c), respectively). No peaks attributable to the preparative reagent [$Cu(NO_3)_2$] or to the copper amine complex [$Cu(NH_3)_4(NO_3)_2$] (figure 7(c)) were detected.

Broad peaks assignable to CuO were observed in the XRD patterns of the catalysts prepared from $Cu(NO_3)_2$ both after activation and after use in the NO reaction (table 2), providing evidence for the formation of microcrystalline CuO. With the catalysts prepared with higher loadings of Cu (40 wt%) after use broad peaks of Cu_2O and/or sharp peaks of metallic Cu were also evident. No peak was observed after the activation of $Cu(NH_3)_4(NO_3)_2$/AC although broad peaks assignable to CuO again appeared after the catalyst was employed in the reaction.

The powder XRD results show that $Cu_2(OH)_3Cl$ is obtained when $CuCl_2$ is employed as a preparative reagent with AC, while $Cu_4SO_4(OH)_6$ and $Cu_3SO_4(OH)_4$ result from the use of $CuSO_4$ (table 2). These supported species are retained on the support after activation (523 K in helium) and use in the NO reduction process, although after the latter the intensities of the XRD peaks for $Cu_2(OH)_3Cl$ have diminished. Although $Cu(CH_3COO)_2$/AC showed no activity for NO reduction, sharp peaks of Cu and Cu_2O but no CuO peaks were observed in the XRD pattern.

The XRD patterns for the CB catalysts were similar to those measured for the AC catalysts with broad peaks of microcrystalline CuO again being seen in the patterns of the active CB catalysts (figure 8). The XRD pattern for 40% $Cu(NO_3)_2$/CB after impregnation displayed two superimposed sets of peaks with slightly different diffraction angles (2θ) (figure 8(c)), indicative of the presence of $Cu_2(OH)_3NO_3$ crystals with dissimilar lattice distances. The crystals with smaller lattices are believed to reside on the outer surface of the support, as will be discussed later in this report. Although $Cu(NO_3)_2$/UC showed no activity for the reduction of NO, broad peaks of CuO were also detected

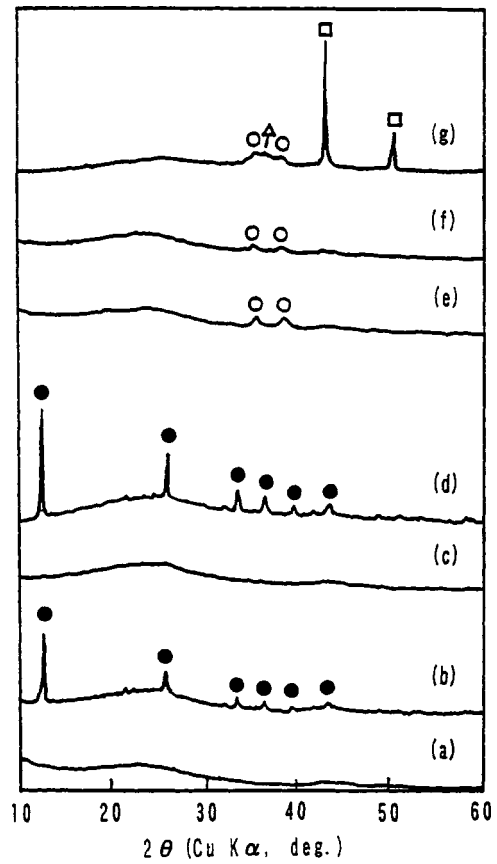

Figure 7. Powder X-ray diffraction patterns of AC (a) and Cu salts-on-AC before (b–d) and after (e–g) use for NO reduction; (b, e) 10% $Cu(NO_3)_2$-on-AC; (c, f) 10% $[Cu(NH_3)_4](NO_3)_2$; (d, g) 40% $Cu(NO_3)_2$; reaction conditions as in figure 3; peak symbols: (●) $Cu_2(OH)_3NO_3$, (○) CuO, (△) Cu_2O, (□) Cu.

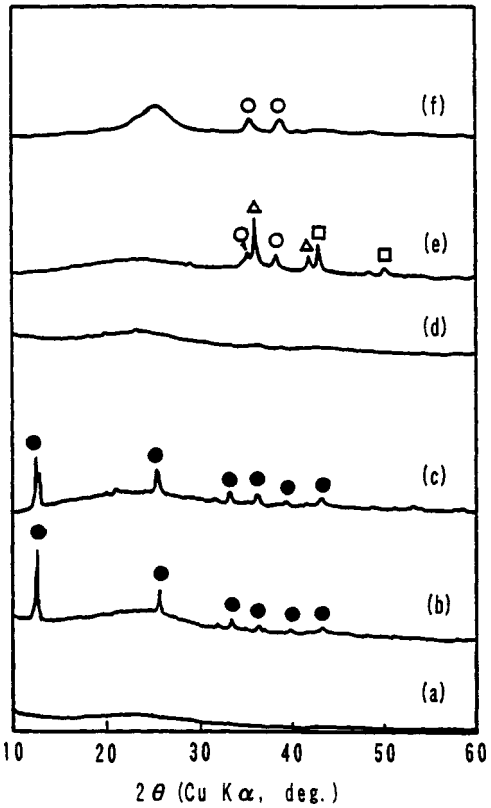

Figure 8. Powder X-ray diffraction patterns of CB (a), Cu-on-CB (b–e) and Cu-on-UC (f) before (b, c) and after (d–f) use for NO reduction; (b, d, f) 10% $Cu(NO_3)_2$; (c, e) 40% $Cu(NO_3)_2$; reaction conditions and peak symbols as in figure 7.

Table 2
XRD analysis for copper and iron salts supported on carbon.

Sample	Crystals detected[a]		
	After impregnation	After activation	After reaction
10% $Cu(NO_3)_2$/AC	$Cu_2(OH)_3NO_3$ (vs)	CuO (b)	CuO (b)
10% $Cu(NH_3)_4(NO_3)_2$/AC	(none)	(none)	CuO (b)
10% $CuCl_2$/AC	$Cu_2(OH)_3Cl$ (s)	$Cu_2(OH)_3Cl$ (vs)	$Cu_2(OH)_3Cl$ (l)
10% $CuSO_4$/AC	$Cu_4SO_4(OH)_6$ (s)[b]	$Cu_4SO_4(OH)_6$ (s)[b]	$Cu_4SO_4(OH)_6$ (s)[b]
	$Cu_3SO_4(OH)_4$ (s)	$Cu_3SO_4(OH)_4$ (s)	$Cu_3SO_4(OH)_4$ (s)
10% $Cu(CH_3COO)_2$/AC	(none)	Cu (vs)	Cu (vs), Cu_2 (b)
40% $Cu(NH_3)_2$/AC	$Cu_2(OH)_3NO_3$ (vs)	CuO (b), Cu_2O (b)	CuO (b), Cu_2O (b), Cu (vs)
10% $Cu(NO_3)_2$/AC[c]	–	–	CuO (b)
10% $Cu(NO_3)_2$/CB	$Cu_2(OH)_3NO_3$ (vs)	–	CuO (b), Cu_2O (b)
40% $Cu(NO_3)_2$/CB	$Cu_2(OH)_3NO_3$ (vs)	CuO (b), Cu_2O (b), Cu (b)	CuO (b), Cu_2O (s), Cu (vs)
10% $Cu(NO_3)_2$/UC	$Cu_2(OH)_3NO_3$ (vs)	–	CuO (b)
10% $Fe(NO_3)_3$/AC	(none)	(none)	(none)
10% $FeCl_3$/AC	(none)	(none)	Fe_2O_3

[a] vs, very sharp; s, sharp; b, broad; l, low intensity.
[b] Unidentified peaks are also present.
[c] Used for NO reduction with NH_3 and O_2.

Table 3
Crystallite size of copper species on various carbon catalysts after used NO reduction with NH_3.

Sample	Crystallite size (nm)		
	CuO(111)	Cu_2O(111)	Cu(111)
10% $Cu(NO_3)_2$/AC	26	–	–
10% $Cu(NH_3)_4(NO_3)_2$/AC	28	–	–
40% $Cu(NO_3)_2$/AC	19	<19	>900
10% $Cu(NO_3)_2$/AC[a]	21	–	–
10% $Cu(NO_3)_2$/CB	33	21	–
40% $Cu(NO_3)_2$/CB	29	210	>900

[a] Used for NO reduction with NH_3 in the presence of O_2.

in the XRD pattern (figure 8(f)). No peaks were detected for $Fe(NO_3)_3$/AC and $FeCl_3$/AC either after the impregnation or after the activation but small peaks due to Fe_2O_3 were seen with $FeCl_3$/AC after use in the NO reaction.

The sizes of the crystallites of CuO were estimated, on average, to be smaller (19 nm) for 40% $Cu(NO_3)_2$/AC than those (26 nm) for the 10% loading of the same catalyst as well as those (28 nm) for 10% $Cu(NH_3)_4(NO_3)_2$/AC (table 3). The crystallite sizes (30 nm) of $Cu(NO_3)_2$/CB were found to be independent of the loading. Large crystallites (>900 nm) of metallic copper were detected in the higher loading (40 wt%) samples prepared from AC and CB, while smaller (<19 nm) and relatively large (210 nm) crystallite sizes of Cu_2O were found in the AC and CB catalysts, respectively.

3.8. Scanning electron microscopy

SEM images of AC manufactured from coals show the presence of distorted cylindrical holes with relatively large diameters (ca. 10 μm) presumably reflecting the shape of cells of fossil plants before carbonization (figure 9(a)). The white aggregates occupying holes of approximately 5 μm in 10% $Cu(NO_3)_2$/AC (figure 9(b)) are identified as crystalline $Cu_2(OH)_3NO_3$ by comparison with the corresponding XRD results (figure 7(b)). Use in the reduction of NO converts these crystals into smaller (2 μm) spheres of CuO, which are dispersed in the holes in AC (figure 9 (c) and (d)). Similar aggregates, which appear to be composed of small clusters, are observed with 10% $Cu(NH_3)_4(NO_3)_2$/AC after use in the NO process. Larger aggregates are evident with the $Cu(NO_3)_2$/AC catalysts of higher loading (40%) (figure 8(h)).

With the CB catalysts the cross sections are relatively undistinguished (figure 10(a)). Rod-like crystallites of $Cu_2(OH)_3NO_3$ are observed with $Cu(NO_3)_2$/CB after impregnation (figure 10(b)). With both 10% and 40% $Cu(NO_3)_2$/CB the crystallites of CuO increase in size and appear more distinctive after use in the reaction (figure 10 (c), (f); cf. figure 10 (b), (e)). From a comparison of figure 10 (c) and (f) it appears that increases in the loading of Cu on CB increase the number of large CuO crystallites rather than the size of the crystals.

It is of interest to compare features contained within the SEM cross sections and outer surface images for the CB catalysts of various loadings. In particular, a mass of large crystallites, assigned to Cu_2O and/or Cu, by reference to the XRD results (figure 8(e)), is deposited on the external surface of 40% $Cu(NO_3)_2$/CB (figure 10(g)). It is possible that the impregnation process leading to the preparation of this heavily loaded catalyst may result in the deposition of copper species on the outer surfaces leading to a relatively low activity for this catalyst.

The SEM image of $Cu(NO_3)_2$/UC reveals a mass of aggregates of crystallites of Cu deposited on a plain external surface (figure 9(h)).

4. Discussion

4.1. State of metal salts supported on carbon

Impregnation of carbons from aqueous solutions of simple copper salts such as the chloride, nitrate and sulfate, followed by drying at 373 K, leads to the formation of the corresponding partial hydroxides. It has been reported that the hydroxynitrate and hydroxychloride can be synthesized from solutions of the nitrate and of the chloride, respectively, by hydrothermal reaction at relatively low temperatures (473–493 K) [39,40]. Thus the formation of the partial hydroxides probably occurs during the drying of solutions of the copper salts and is not specific to the impregnation of carbons. The present SEM observations on the impregnated carbons clearly show, as expected in view of the hydrophobic nature of the surface of carbons, that the partial hydroxides occupy the large holes (5 μm) of AC, as previously reported for K_2CO_3/AC [41]. Relatively large crystals of partial hydroxides of $Cu(NO_3)_2$ were also observed on the CB support, as would be expected if the aqueous solutions tend to migrate to the wider pores in hydrophobic porous materials. With CB catalysts of higher loading of Cu (e.g., 40%) significant quantities of copper salts were deposited on the outer surface of the particles of the support, resulting in lower activity for NO reduction. In contrast, with the amine complex of $Cu(NO_3)_2$ and copper acetate on AC no distinctive XRD peaks were evident, suggesting relatively high dispersions of the supported materials or the formation of amorphous copper compounds on the support.

Heat treatment (523 K in He) of $Cu_2(OH)_3NO_3$ on AC or CB results in the formation of CuO with crystallite sizes of ca. 20 and 30 nm, respectively. With the activated CB catalysts of higher Cu loading (40%), XRD peaks assigned to Cu_2O and metallic Cu, apparently deposited on the outer surface of the support, were observed. With copper acetate/AC after heat treatment sharp XRD peaks associated with large crystallites of metallic Cu were present. This may result from the reduction of Cu^{2+} to Cu followed by growth of crystals of the latter. Since no peaks appeared for $Cu(NH_3)_4(NO_3)_2$/AC the copper compound, presumably CuO, is highly dispersed on the support.

With the used AC and CB catalysts with higher Cu loading (40%) Cu_2O and/or metallic Cu was observed after use

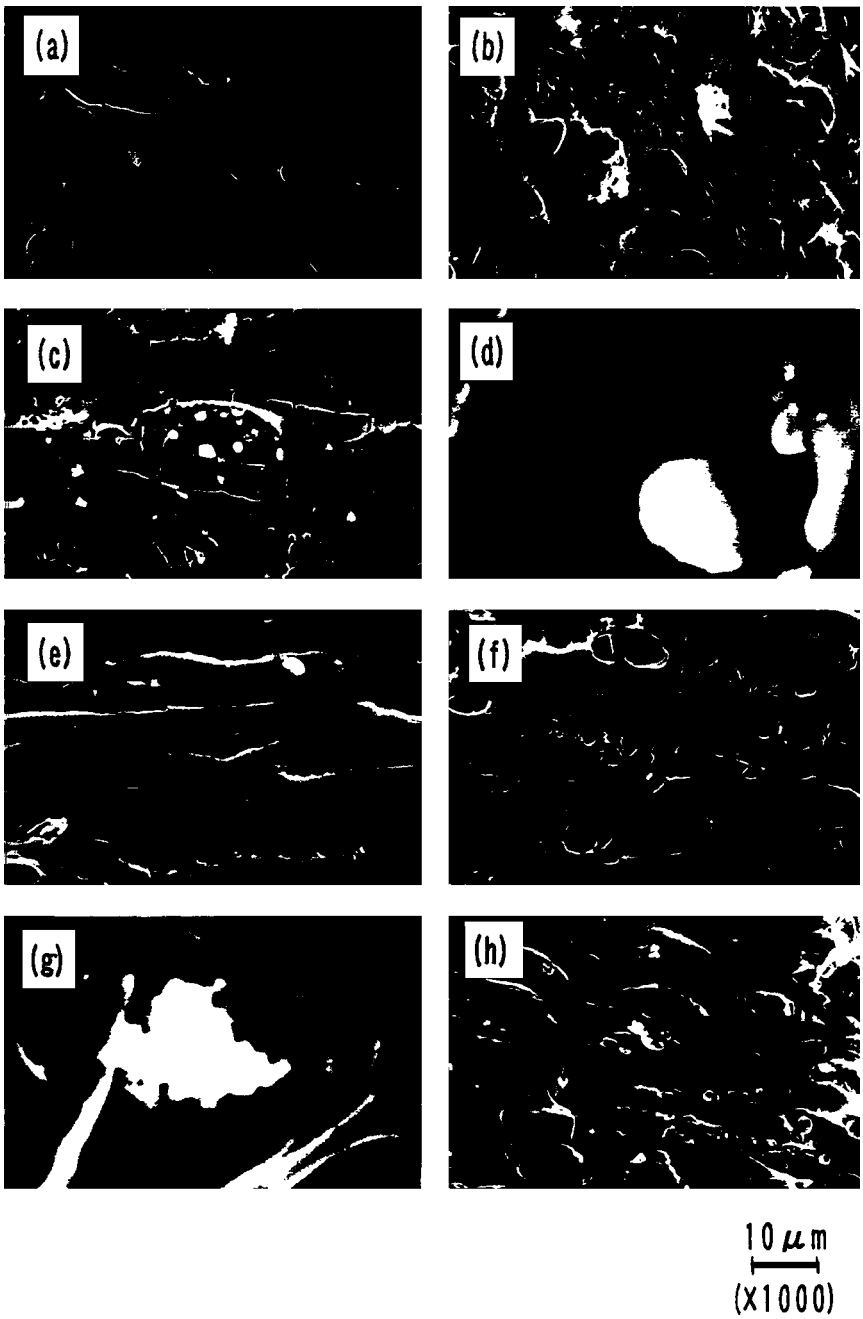

Figure 9. Cross-sectional SEM images of AC (a) and Cu-on-AC before (b, e) and after (c, d, f–h) use for NO reduction; (d, g) ×10000; (other) ×1000; (b–d) 10% $Cu(NO_3)_2$; (e–g) 10% $[Cu(NH_3)_4](NO_3)_2$; (h) 40% $Cu(NO_3)_2$; reaction conditions as in figure 3.

of the catalysts, in agreement with the results reported by others for NO reduction by NH_3 over CuO [42]. In contrast, microcrystalline CuO remained on 10% $Cu(NO_3)_2$/carbon after use in the reaction. With used $Cu(NO_3)_2$/AC small spherical aggregates of microcrystalline CuO were found on the walls of relatively large holes in the support while on the CB support the CuO appeared in the form of cylinders.

The aforementioned differences in the composition and form of the supported species may be correlated with the activities in the reduction of NO. The larger holes in AC, in comparison with the absence of porosity in CB, would be expected to favour transport of reactant and product gases and to facilitate contact of the reactant gas with the active species deposited on the walls of the channels. The third carbonaceous support (UC), with a relatively small surface area and low dispersion of the supported material on the peripheral surface of UC, was, as expected, less active in the reduction process.

It is of interest to note that the activity of Cu/ZSM-5 catalysts in the reduction of NO has been related to the presence of copper [43] and CuO and Cu_2O [44–46] aggregates on the outer surface of the zeolite. Recent characterization studies on amorphous and graphitic forms of carbon have

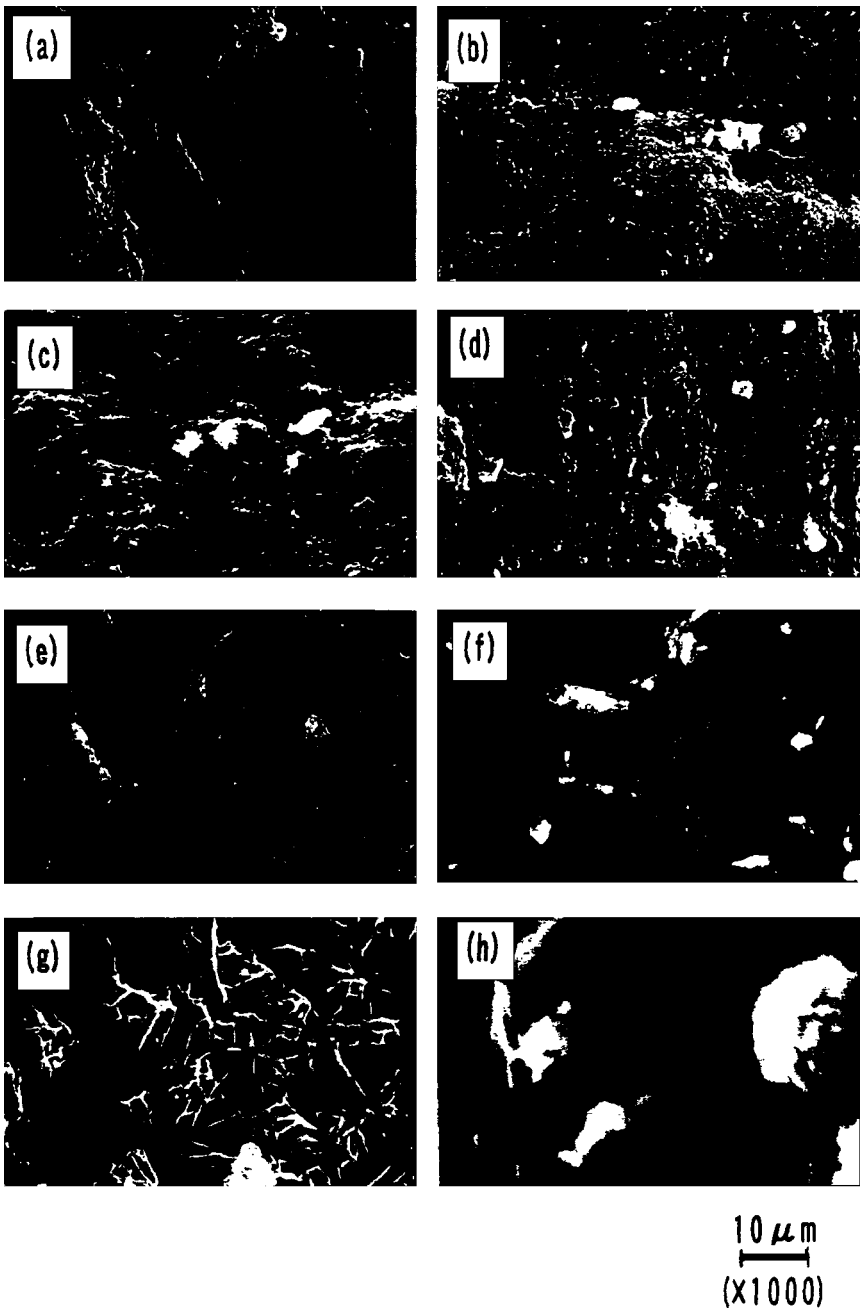

Figure 10. Cross-sectional (a–c, e, f, h) and outer surface (d, g) SEM images of CB (a) and Cu-on-CB before (b, e) and after (c, d, f, g) use for NO reduction; (h) ×10000; (other) ×1000; (b–d) CB; (b) 10% $Cu(NO_3)_2$; (e–g) 40% $Cu(NO_3)_2$; (h) 10% $Cu(NO_3)_2$-on-UC after use; reaction conditions as in figure 3.

tentatively identified Cu_2O as the stable chemical state of Cu on amorphous and graphitic forms of carbon at moderate temperatures and under reducing conditions [33].

4.2. Active copper species

Of the four cations examined the order of activity for the conversion of NO to N_2 at 450 K is $Cu > Fe > Co > Ni$, consistent with the increase in the stability of the ion of lesser oxidation state relative to that of higher oxidation state. Since with Cu the conversion of NO increases as the loading increases in the order $AC > CB > UC$, it is tempting to relate this primarily to the surface areas which follow the same order. However, it is to be noted that at a loading of 40% the conversions with AC, CB and UC are approximately 81, 20 and 5%, respectively, while the surface areas are 1576, 1270 and 21 m^2/g, respectively. Thus while morphological factors are undoubtedly important in the NO reduction process and indeed high surface areas are probably necessary, but not sufficient, other properties must certainly play a role.

Of the catalysts examined in the present work, those which displayed appreciable activities in the reduction process contained microcrystalline CuO. Consequently it

seems reasonable to conclude that these are either the active species in the reduction process or the precursors to such species. Similar conclusions have been drawn for other copper catalysts prepared with a variety of supports [42,47] as well as with Cu/ZSM-5 [46].

Although a variety of mechanisms has been suggested to explain the activity of Cu/ZSM-5 in the NO reduction process, a number of authors have concluded that NO is first oxidized to NO_2 which then interacts with the reductant [48–53]. Since in the present work the introduction of O_2 has a profound effect on the activity of $Cu(NO_3)_2$/AC, yielding 100% conversion at temperatures as low as 175 °C, the possibility of such a mechanism cannot be eliminated with the present catalysts. The relatively small improvement in conversion of $Cu(NO_3)_2$/AC after partial deactivation followed by exposure to oxygen suggests that oxygen plays a more important role with the reactant than with the surface.

In view of the observation with H-ZSM-5 catalysts that NO_2 is more easily reduced than NO it appears reasonable to conclude that the oxidation of NO is the first step in the overall process [48–53]. Further, since the homogeneous oxidation of NO to NO_2 is slow while that on Cu-ZSM-5 is rapid compared to H-ZSM-5, it appears that the oxidation process is occurring on copper sites [54]. That the activity of NO oxidation parallels the activity for the generation of N_2 provides further evidence for the involvement of NO_2 as an intermediate.

With the catalyst showing the highest activity (40% $Cu(NO_3)_2$/AC) in the absence of oxygen, CuO, Cu_2O and metallic Cu were detected after use, while only CuO was found on the same catalyst with 10% loading. Monovalent copper has been favoured as an active site with Cu/ZSM-5 [55,56], while the importance of the bivalent species has also been emphasized [50,57,58]. Most recent studies with the decomposition of NO over Cu-ZSM-5 suggest that the addition of a reducing agent (in this work, CO) promoted the reduction of Cu^{2+} to Cu^{+} [59]. The simplest scheme for the rationalization of the present results thus involves the oxidation of NO on Cu^{2+} sites,

$$NO + 2CuO \rightarrow NO_2 + Cu_2O \quad (1)$$

with the NO_2 subsequently reduced by NH_3,

$$3NO_2 + 4NH_3 \rightarrow 3\tfrac{1}{2}N_2 + 6H_2O \quad (2)$$

while the Cu^{2+} sites are regenerated by NO_2,

$$NO_2 + 2Cu_2O \rightarrow \tfrac{1}{2}N_2 + 4CuO \quad (3)$$

With the catalysts of higher copper loading the CuO supported on the external surface was reduced to Cu via Cu_2O,

$$3Cu_2O + 2NH_3 \rightarrow N_2 + 3H_2O + Cu \quad (4)$$

while, in the presence of O_2, CuO was directly regenerated with O_2 from Cu_2O,

$$2Cu_2O + O_2 \rightarrow 4CuO \quad (5)$$

There is no evidence, from the present work, of the direct participation of the support in the mechanism of the process although, as noted earlier in this report, the support appears to be playing more than a morphological role.

Acknowledgement

The financial support of the Natural Sciences and Engineering Research Council of Canada is gratefully acknowledged.

References

[1] R.M. Heck and R.J. Farrauto, *Catalytic Air Pollution Control* (Van Nostrand Reinhold, New York, 1995).
[2] J. Armor, *Environmental Catalysis*, ACS Symposium Series, Vol. 552 (Am. Chem. Soc., Washington, DC, 1994).
[3] H. Bosch and F. Janssen, Catal. Today 2 (1988) 369.
[4] G.C. Bond and S.F. Tahir, Appl. Catal. 71 (1991) 1.
[5] *Canada's Second National Report on Climate Change: Actions to Meet Commitments under the United Nations Framework Convention on Climate Change* (Environment Canada, Ottawa, May 1997).
[6] A.M. Efstathion and K. Fliatoura, Appl. Catal. B 6 (1995) 35.
[7] S. Hu and T.M. Apple, J. Catal. 158 (1996) 199.
[8] R.M. Heck, J.M. Chen and B.K. Speronello, Envir. Prog. 13 (1994) 221.
[9] N.-Y. Topsøe, H. Topsøe and J.A. Dumesic, J. Catal. 151 (1995) 226.
[10] N.-Y. Topsøe, J.A. Dumesic and H. Topsøe, J. Catal. 151 (1995) 241.
[11] N.-Y. Topsøe, Science 265 (1994) 1217.
[12] B. Herrlander, Catal. Today 4 (1989) 219.
[13] K.C. Taylor, in: *Catalysis and Automotive Pollution Control*, eds. A. Crucq and A. Frennet (Elsevier, Amsterdam, 1987) p. 97.
[14] P. Marécot, L. Perault, G. Mabilan, M. Prigent and J. Barbier, Appl. Catal. B 5 (1994) 57.
[15] S.E. Golumski, H.A. Hatcher, R.R. Rajaram and T.J. Truex, Appl. Catal. B 5 (1995) 367.
[16] L. Singoredjo, M. Slagt, J. van Wees, F. Kapteijn and J.A. Moulijn, Catal. Today 7 (1990) 157.
[17] L. Singoredjo, R. Korver, F. Kapteijn and J. Moulijn, Appl. Catal. B 1 (1992) 297.
[18] G. Centi, C. Nigro, S. Perathoner and G. Stella, Catal. Today 17 (1993) 159.
[19] A. Kato, S. Matsuda and T. Kamo, Ind. Eng. Chem. Prod. Res. Dev. 22 (1983) 406.
[20] G. Centi, S. Perathoner, D. Biglino and E. Giamello, J. Catal. 151 (1995) 75.
[21] G. Centi and P. Forzotti, *Environmental Catalysis*, Catal. Today 27 (1996) 1.
[22] E. Richter, Catal. Today 7 (1990) 93.
[23] H. Juntgen, E. Richter and H. Kuhl, Fuel 67 (1988) 775.
[24] A. Nishijima, Y. Kiyozumi, A. Ueno, M. Kurita, H. Hagiwara, T. Sato and N. Todo, Bull. Chem. Soc. Jpn. 52 (1979) 3724.
[25] F. Nozaki, K. Yamazaki and T. Inomata, Chem. Lett. (1977) 521.
[26] T. Grzybek, Fuel 69 (1990) 604).
[27] T. Grzybek and H. Papp, Appl. Catal. B 1 (1992) 271.
[28] T. Grzybek, Fuel 72 (1993) 619.
[29] A. Nishijima, M. Kurita, Y. Kiyozumi, R. Kobayashi, H. Hagiwara, A. Ueno, T. Sato and N. Todo, Bull. Chem. Soc. Jpn. 53 (1980) 3356.
[30] S. Kasaoka, E. Sasaoka and H. Iwasaki, Bull. Chem. Soc. Jpn. 62 (1989) 1226.
[31] P. Ehrburger and J. Lahaye, in: *Petroleum-Derived Carbons*, ACS Symposium Series, Vol. 303, eds. J.D. Bacha, J.W. Newman and J.L. White (Am. Chem. Soc., Washington, DC, 1986) p. 310.

[32] C. Marquez-Alvarez, I. Rodriguez-Ramos and A. Guerrero-Ruiz, Carbon 34 (1996) 1509.
[33] J. Ma, N.M. Rodriguez, M.A. Vannice and R.T.K. Baker, J. Catal. 183 (1999) 32.
[34] A. Dandekar, R.T.K. Baker and M.A. Vannice, J. Catal. 183 (1999) 131.
[35] J.J. Bikerman, *Physical Surfaces* (Academic Press, New York, 1970) p. 274.
[36] M. Kakudo and N. Kasai, *X-Ray Diffraction by Polymers* (Kodansha, Tokyo, 1972) p. 329.
[37] R.W. Cranston and F.A. Inkley, Adv. Catal. 9 (1957) 143.
[38] L. Lietti, I. Nova, G. Ramis, L. Dall'Acqua, G. Busca, E. Giamello, P. Forzatti and F. Bregani, J. Catal. 187 (1999) 419.
[39] H. Effenberger, Z. Kristallogr. 165 (1983) 127.
[40] H.R. Oswald and W. Feitknecht, Helv. Chim. Acta 47 (1964) 272.
[41] S. Hirano, N. Shigemoto, S. Yamada and H. Hayashi, Bull. Chem. Soc. Jpn. 68 (1995) 1030.
[42] K. Otto and M. Shelef, J. Phys. Chem. 76 (1972) 37.
[43] J.O. Petunchi, G. Sill and W.K. Hall, Appl. Catal. B 2 (1993) 122.
[44] E.S. Shpiro, W. Grunert, R.W. Joyner and J.N. Baeva, Catal. Lett. 24 (1994) 159.
[45] W. Grunert, N.W. Hayes, R.W. Joyner, E.S. Spiro, M.R.H. Siddigui and G.N. Baeva, J. Phys. Chem. 98 (1994) 10832.
[46] C.M. Marques-Alvarez, I. Rodrigues-Ramos, M. Gernandes-Garcia and G.L. Haller, in: *Proc. 11th Int. Congr. on Catal.*, eds. J.W. Hightower, W.N. Delgass, E. Iglesia and A.T. Bell (Elsevier, Amsterdam, 1996) p. 206.
[47] T. Iizuka, H. Ikeda and S. Okazaki, J. Chem. Soc. Faraday Trans. I 82 (1986) 61.
[48] H. Hamada, Y. Kitaichi, M. Sasaki and T. Ito, Appl. Catal. 70 (1991) L15.
[49] H. Hamada, Y. Kintaichi, M. Sasaki, T. Ito and M. Tabata, Appl. Catal. 75 (1991) L1.
[50] J.O. Petunchi and W.K. Hall, Appl. Catal. B 2 (1993) 1205.
[51] J. Valyon and W.K. Hall, Appl. Catal. B 2 (1993) L17.
[52] G. Centi, S. Perattoner, D. Biglino and E. Giamello, J. Catal. 151 (1995) 75.
[53] V.A. Sadykov, S.L. Baron, V.A. Matyshak, G.M. Alikina, R.V. Bunina, A.Ya. Rozovskii, V.V. Lunin, E.V. Lunina, A.N. Kharlanov, A.S. Ivanova and A.S. Veniaminov, Catal. Lett. 37 (1996) 157.
[54] M. Shelef, C.N. Montreuil and H.-W. Jen, Catal. Lett. 26 (1994) 277.
[55] M. Iwamoto, presented at the ACS Meeting, 1993, paper 23.
[56] B.K. Cho, J. Catal. 155 (1995) 184.
[57] G.P. Ansell, A.F. Diwail, S.E. Golunski, J.M. Hayes, R.R. Rayaram and A.P. Walker, Appl. Catal. B 1 (1992) 1.
[58] A. Kucherov, J.L. Gerlock, H.-W. Jen and M. Shelef. J. Catal. 152 (1995) 63.
[59] M.V. Konduru and S.S.C. Chuang, J. Catal. 187 (1999) 436.